ISIJ International, Vol. 38 (1998), No. 9, pp. 959–966

Experimental Studies of Interfacial Heat Transfer and Initial Solidification Pertinent to Strip Casting

Les STREZOV and Joe HERBERTSON

Centre for Metallurgy and Resource Processing, BHP Research, Newcastle, PO Box 188, Wallsend, NSW 2287, Australia.

(Received on February 2, 1998; accepted in final form on April 24, 1998)

Melt/substrate contacting experiments have been carried out under controlled laboratory conditions designed to approximate the conditions encountered during the initial solidification period in strip casting. Immersion experiments were performed with various substrates embedded in a moving paddle; the substrates had both smooth and textured surfaces. The melt was 304 austenitic stainless steel, and the substrates were made from copper blocks. The apparatus and instrumentation were designed for 'millisecond' resolution of heat transfer behaviour. The experimental variables chosen for study were substrate texture, gas atmosphere, immersion velocity and melt superheat. The conclusions drawn were based on an analysis of transient interface heat fluxes during the first 50 milliseconds of contact, the observed nucleation behaviour and the resultant surface and internal solidification structures. The aim of the work was to add to the fundamental understanding of melt/substrate contacting in the meniscus region, since this will inevitably be critical to strip surface quality.

KEY WORDS: strip casting; interfacial heat transfer; initial solidification; stainless steel.

1. Introduction

Over the past decade or so, there has been intensive research activities to develop a commercial technology for direct casting of steel strip, mainly using twin roll casters. A schematic representation of a twin roll caster[1] is shown in **Fig. 1**. Unlike conventional continuous casting, strip casting is carried out without mould flux and solidification proceeds rapidly as a result of the direct contact between liquid steel and the mould [substrate] surface. As a consequence, much higher initial heat transfer rates are an inherent challenge in twin roll casting conditions. Furthermore, the surface area to volume ratio is typically two orders of magnitude greater than slab casting, making good surface quality a precondition for the successful implementation of this technology. Better fundamental understanding of heat transfer and solidification processes taking place at the metal/substrate interface therefore becomes of paramount importance in controlling the surface and internal quality of the strip. This presents a major experimental challenge, given the complexity of the phenomena taking place within a small fraction of a second.

Melt/substrate contact commences at the meniscus and is established by mechanisms of dynamic wetting. Heat transfer at the metal/substrate interface is by conduction through the points of intimate contact, plus radiation, convection and conduction across any entrapped gas in the interfacial 'gap'. Using a laboratory scale twin roll caster, which employed copper rolls to cast austenitic stainless steel, Miyazawa, Mizoguchi and co-workers[2,3] have observed an increase in the overall melt/roll heat transfer coefficient with increasing casting velocity. This was attributed to a reduction in thickness of the layer of trapped gas at the interface. Using a mathematical approach, the effects of casting velocity, melt superheat, gas and slag films on the melt/roll interface heat transfer coefficient were examined. The melt/roll heat transfer coefficient was shown to be affected by the gas composition at the interface.[4] Increasing casting velocity was shown to have a beneficial effect on the strip surface quality.[5] Further experimental work on stainless

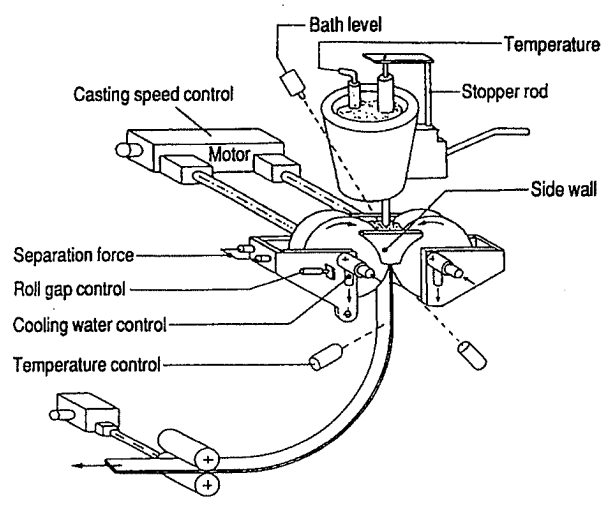

Fig. 1. Schematic representation of a twin roll caster.[1]

steel strip casting, carried out by Grosjean *et al.*[6] on a prototype twin roll caster, has demonstrated the importance of substrate texture. The average heat flux was shown to decrease significantly with roll surface roughness. The above studies measured the overall, average heat exchange between the pool melt and the rolls, not the transient heat flux as a section of the roll surface contacts the meniscus and is immersed in the melt pool.

In the closely related field of rapid solidification of ultra-thin ribbons and amorphous metals, the most important parameters controlling melt/substrate heat transfer rates have been shown to be the substrate surface chemistry, texture, temperature and velocity, as well as the melt superheat and chemistry and the ambient atmosphere.[7] Substrate texture can have a particularly strong effect on the surface and sub-surface solidification structures. For example in a study of Al–Cu alloys, for a wide range of substrate materials, the same substrate roughness conditions resulted in very similar surface and sub-surface solidification structures.[8] Moreover, the nucleation sites were aligned with the edges of the machined grooves in the substrates.

For heat transfer problems such as these, where the boundary conditions at the surface are not known, inverse numerical techniques can be used to estimate the interfacial heat transfer rates, based on temperature measurements taken from the substrate interior. When the interface heat flux is changing rapidly, as is the case here, the inherent thermocouple sensor dynamics can also introduce errors if not controlled and optimised.[9] The most common technique to calculate interfacial heat fluxes is to use the finite difference method, which was first proposed by Beck *et al.*[10] and has since been adopted by many other workers in the field. A modified version of Beck's IHCP algorithm [inverse heat conduction problem] was used in this study.

In the present work, melt/substrate contacting experiments were carried out under controlled laboratory conditions designed to approximate the conditions encountered during the initial solidification period in strip casting. The melt was 304 austenitic stainless steel, and the substrates were made from copper. The aim of the work was to add to the fundamental understanding of melt/substrate contacting near the meniscus, as phenomena taking place in this region are bound to play a critical role in determining strip quality.

2. Experimental Details

Melt immersion experiments were performed with various substrates embedded in a moving paddle, which was inclined at an angle similar to the melt/roll contacting geometry of the meniscus region of a twin roll caster. The apparatus and instrumentation were designed for 'millisecond' resolution of heat transfer behaviour. The experimental variables chosen for study were substrate texture, gas atmosphere, immersion velocity and melt superheat. The conclusions drawn were based on an analysis of transient interface heat fluxes during the first 50 milliseconds of contact, the observed nucleation behaviour and the resultant surface and internal solidification structures.

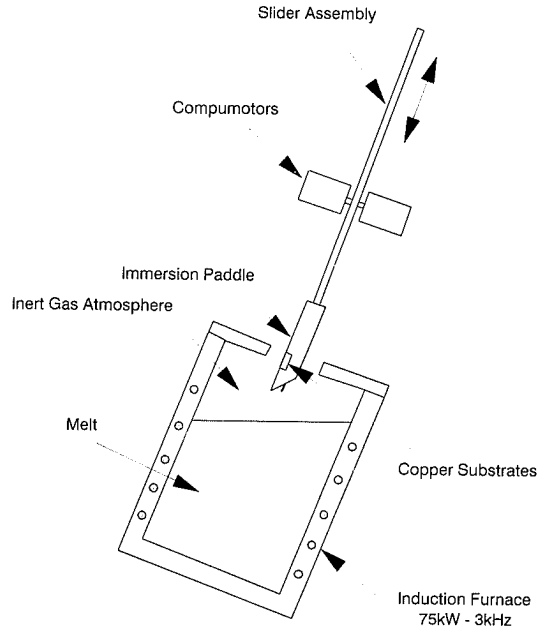

Fig. 2. Schematic representation of the experimental apparatus.

Table 1. Melt composition. (wt%)

	C	Mn	Si	S	Ni	Cr
Min.	.056	1.00	.38	.019	8.8	17.85
Max.	.060	1.05	.42	.022	9.0	18.00

2.1. Procedures

The apparatus, shown schematically in **Fig. 2**, was used to produce cast metal samples under controlled immersion conditions and to record the associated temperature increase in the substrates. The melt phase composition, corresponding to 304 austenitic stainless steel, is given in **Table 1**. A positive pressure of argon was maintained above the melt, thus creating an inert gas atmosphere. In some experiments helium or argon–helium gas mixtures were used. The immersion velocity profile was controlled by two computer controlled electric motors. The paddle was accelerated through the melt surface to the prescribed casting velocity and travelled at constant speed during the time that the substrates were in contact with the meniscus of the melt. The paddle was then retracted from the melt, to its home position above the furnace, where the solidified samples were removed for examination. The paddle was designed for simultaneous immersion of three substrates with different surface conditions. The substrate blocks were made from $38 \times 38 \times 18.5$ mm electrolytic tough pitch copper. Polishing the substrate surface with number 1 200 emery paper produced a smooth surface finish of about 0.15 μm R_a. Textured substrate surfaces were produced by machining ridges parallel to the immersion direction at a defined pitch and depth, with a tolerance of $\pm 5\,\mu$m. The surfaces of the solidified samples were examined in the as cast condition for nucleation density and surface

solidification structures. Transverse sections were prepared to reveal the internal solidification structures.

Preliminary immersion experiments had shown that after each immersion the substrate surface was coated with a thin layer of grey coloured powder. Analysis of the powder determined it was mainly composed of manganese and silicon based oxides. In order to eliminate the interference of this layer with the results, the substrates were brushed clean prior to each immersion. A subsequent study, to be published separately, was directed at understanding the behaviour of surface oxides.

2.2. Temperature and Heat Transfer Measurements

Two 0.25 mm diameter, type K thermocouples were placed with precision within each substrate block to monitor the temperature close to the surface during immersion. The response rates of the thermocouples [40×10^3 K/s] and the acquisition system [100×10^3 K/s] compared favourably with the maximum rate of temperature rise measured during the initial stage of immersion [$5–15 \times 10^3$ K/s]. During immersion, the substrate temperature acquisition rate was 2 kHz per channel. The output from the thermocouples was sent for analog-to-digital conversion and the data was stored in the computer hard disk. From these data, a period of fifty milliseconds was extracted, beginning at the point in time when the substrate reached the melt meniscus, as manifested in a sharp temperature rise in the substrate thermocouples. The noise present in the raw data was filtered using a polynomial regression method. The transient interface heat flux pattern over the first 50 milliseconds of melt/substrate contact was then calculated using a modified version of Beck's inverse heat conduction algorithm.[10)]

The thermocouples for all the experiments were placed at a depth of 500 to 600 μm below the substrate surfaces. If thermocouples were placed too close to the surface of the substrate, the temperature readings would be highly sensitive to the very localised surface wetting and roughness conditions, giving rise to errors in the estimates of the overall heat flux across the surface at that time. Thermocouples placed further below the substrate surface, where the temperature distribution parallel to the surface would become progressively more uniform, would yield a closer approximation to the overall heat flux across the interface. However, the further a thermocouple were placed below the surface, the less sensitive it would become to the rapidly changing interface heat flux behaviour in the initial period of contact. In order to evaluate the optimum thermocouple position, a two dimensional heat transfer model, with a random heat flux distribution applied across the surface nodes, was used to numerically generate temperature values across the surface and within the substrate. The model generated data were then used to inversely calculate the total surface heat flux using the one-dimensional inverse heat transfer model. The minimum errors [less than 0.5%] were found to be for thermocouples placed at a depth of 500 to 600 μm.

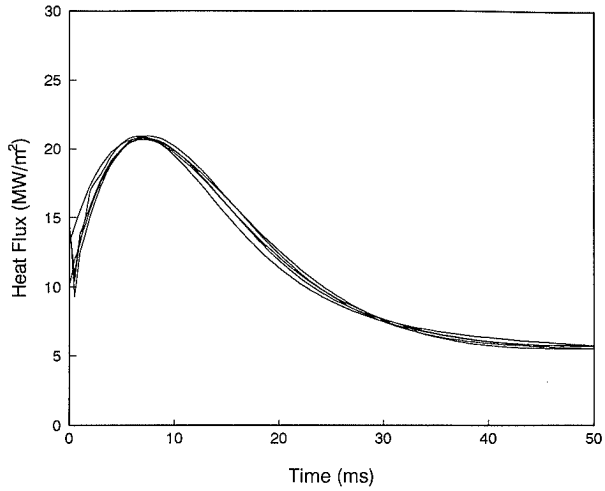

Fig. 3. Reproducibility of heat flux data from five consecutive immersions; textured substrate [150×30 μm], 75 degrees melt superheat, 0.5 m/s immersion velocity, argon atmosphere.

2.3. Reproducibility

In order to check for reproducibility, each experiment was repeated five times. The calculated heat flux data were compared and one of the heat flux curves was accepted as the result for the particular experimental conditions. If the curves did not demonstrate reproducibility, a fresh set of five immersion experiments was conducted. A typical family of curves showing the heat fluxes of five repetitive immersions is presented in **Fig. 3**. These curves show how the heat flux rose to a maximum value over the first ten milliseconds or so, which was the critical period for melt/substrate contact to be established. This behaviour was found to be typical under different experimental conditions, and it proved useful to characterise each experiment by the maximum heat flux, as a quantitative reflection of the effectiveness of initial melt/substrate contact. The reproducibility criteria for a set of five immersion experiments was a variation of less than ± 0.25 MW/m^2 in the maximum heat fluxes and less than ± 2 MW/m^2 for the overall shape of the heat flux curves after the maximum heat flux. Spikes sometimes appeared in the calculated heat flux values within the first two milliseconds, but these were instabilities in the first three time steps of the computational process, not real fluctuations in contacting conditions.

3. Results and Discussion

3.1. Substrate Surface Texture

Substrates selected for these experiments had either smooth or textured surfaces. The textured surfaces had ridges of varying pitch, ranging from 75 to 300 μm, with a constant depth of 30 μm, as shown in **Fig. 4** and **Table 2**. For these experiments, the immersion velocity was constant at 0.5 m/s, an argon atmosphere was used throughout, and the superheat was maintained at 75 degrees.

Figure 5 shows the calculated heat flux histories for the initial 50 milliseconds of contact and solidification on the various substrate surfaces. The maximum heat

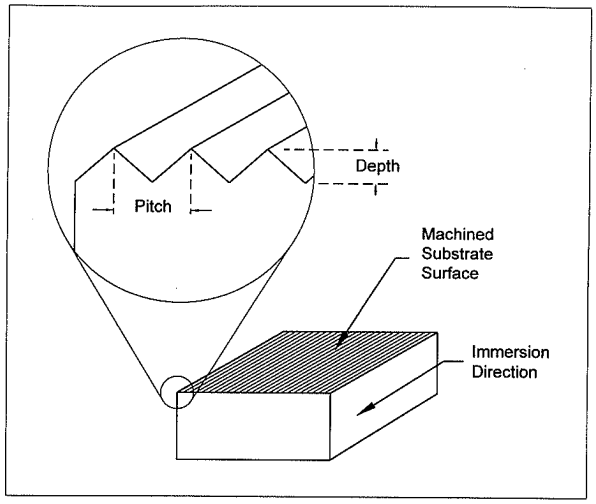

Fig. 4. Schematic of substrate surface texture showing machined ridges parallel to the immersion direction.

Table 2. Substrate surface textures.

No.	Pitch (μm)	Depth (μm)
1	Smooth	$0.15R_a$
2	75	30
3	100	30
4	150	30
5	200	30
6	300	30

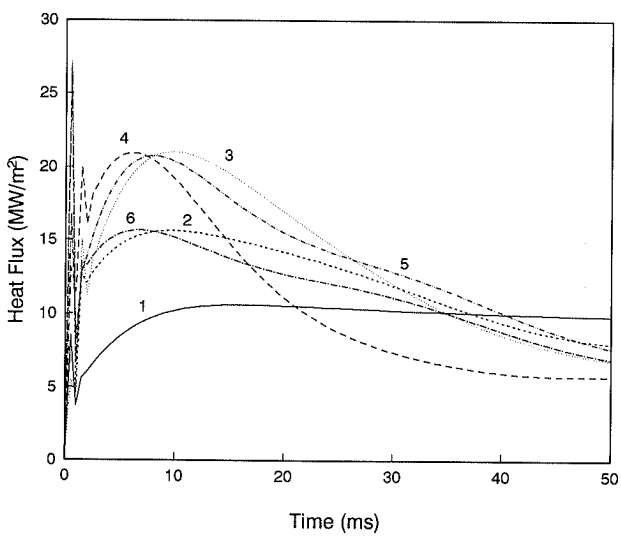

Fig. 5. Heat flux histories for samples solidified on various substrate surfaces; texture details given in Table 2.

flux values were typically reached in about the first 10 milliseconds. The peak heat flux for the smooth substrate was significantly lower than for the textured substrates. **Figure 6** shows how the maximum heat flux varied with texture. The highest values were obtained with ridge pitches between 100 and 200 μm.

Surface solidification structures for the smooth and textured substrates demonstrated quite different nucleation patterns. The surface structure of the samples solidified on the smooth substrate exhibited coarse surface dendrites, with a correspondingly coarse nucleation spacing, as seen in **Fig. 7**. In contrast, the surface structures of the samples solidified on the textured substrates exhibited a definite pattern of nucleation clearly aligned with the ridges machined in the substrates. Fine surface dendrites nucleated along the ridges of the substrate texture, growing perpendicular to the ridge. This is illustrated in **Fig. 8** for the particular case of a 200 μm pitch between the ridges; similarly aligned surface structures were observed with all the ridge textures.

Four areas from the surface of each sample were randomly selected for nucleation frequency counting.

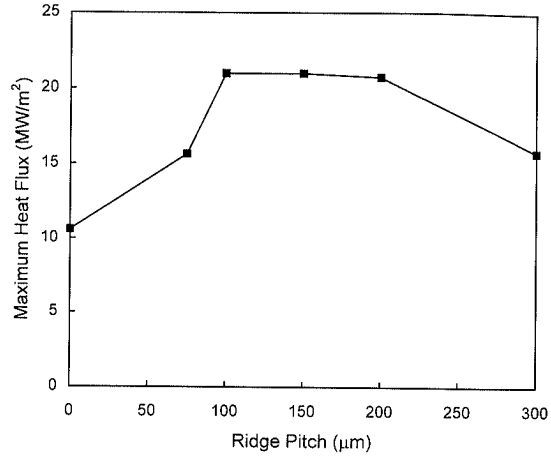

Fig. 6. The effect of substrate surface texture on the maximum heat flux; zero ridge pitch denotes the smooth substrate.

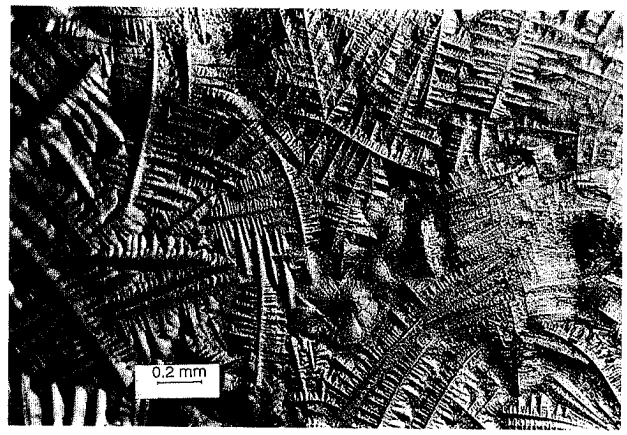

Fig. 7. Surface solidification structure of a sample solidified on the smooth substrate surface.

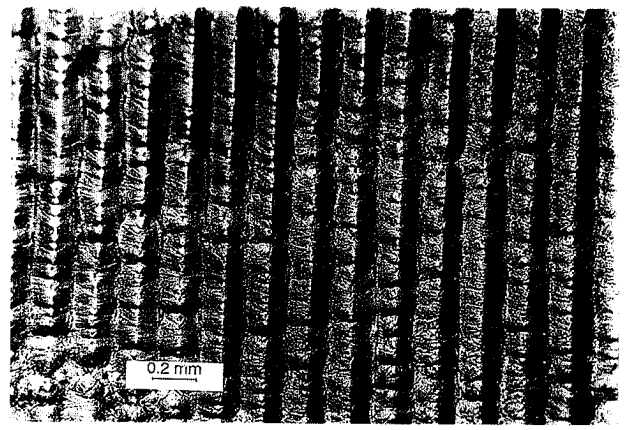

Fig. 8. Surface solidification structure of a sample solidified on a textured substrate surface [200 μm ridge pitch].

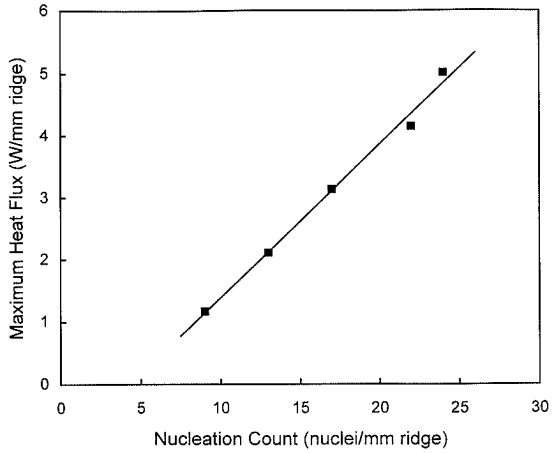

Fig. 9. The effect of nucleation along the ridge on the maximum heat flux.

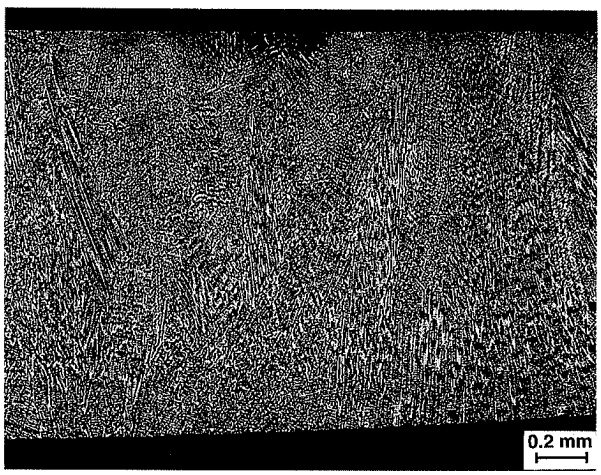

Fig. 10. Transverse solidification structure of a sample solidified on the smooth substrate surface [top surface in contact with substrate].

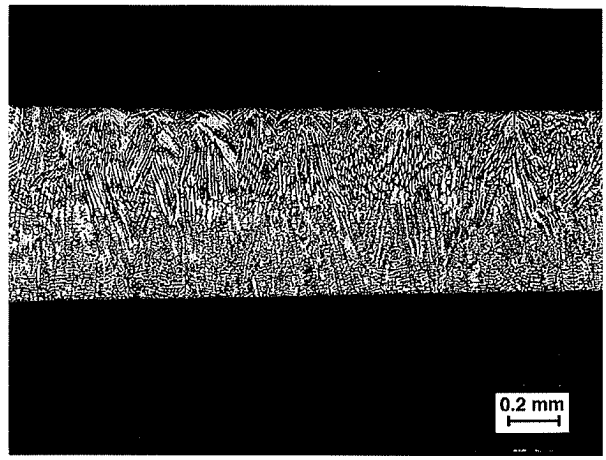

Fig. 11. Transverse solidification structure of a sample solidified on a textured substrate surface [200 μm ridge pitch; top surface in contact with substrate].

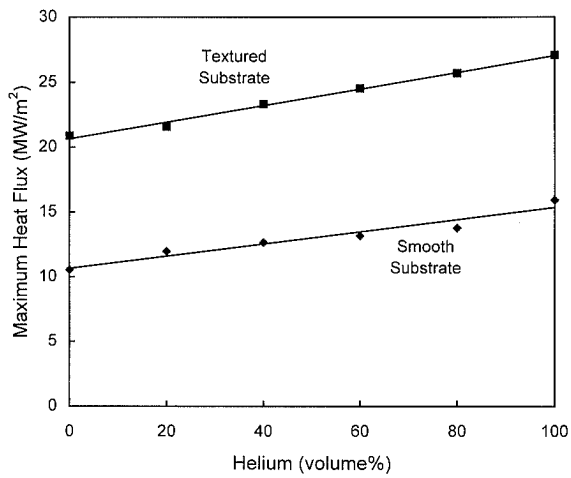

Fig. 12. The effect of helium content on the maximum heat flux for smooth and textured substrates.

The averaged nucleation count from each sample was expressed as nuclei per millimetre of ridge length. Nucleation density for the full range of ridge textures correlated strongly with the peak heat flux data [Fig. 6], when normalised on a ridge length basis. **Figure 9** shows that the maximum heat flux per unit length of ridge increased linearly with the nucleation count along the ridges. Clearly, substrate surface texture has a strong influence on the initial heat flux by controlling the nucleation rate and, by inference, the effectiveness of direct melt/substrate contacting during the first 10 milliseconds or so of immersion below the meniscus.

Transverse microstructures (*i.e.* cross sections in the plane normal to the casting direction) of samples solidified on the smooth and a textured substrate surface [200 μm pitch] are presented in **Figs. 10** and **11**. The solidification structures of all the samples examined were fine in the vicinity of the surface in contact with the chilled substrate and became progressively coarser as a fully columnar growth was established away from the melt/substrate interface. With the textured substrates, the columnar dendrites tended to be coarser with increasing ridge pitch. Although the initial heat fluxes (0–40 ms) with the textured surface was higher than with the smooth surface (Fig. 5), the total heat transferred over the full immersion time was actually higher for the smooth substrate, as evident from the greater sample thickness in Fig. 10.

3.2. Gas Atmosphere

In these experiments, the helium content of the inlet gas to the furnace was varied between 0 to 100% in order to enhance the thermal conductivity of any gas at the melt/substrate interface. The two substrates selected for these experiments were smooth and textured with a 200 μm ridge pitch. The immersion velocity was constant at 0.5 m/s and the superheat was maintained at 75 degrees. Heat flux behaviour was calculated for the first 50 milliseconds, with outputs similar in form to those shown above in Figs. 3 and 5. The results are summarised in **Fig. 12**, where the maximum heat flux observed during initial contact is plotted as a function of the helium content of the gas phase.

The peak heat fluxes were consistently higher with the textured substrate than with the smooth substrate surface, by a relatively constant increment of about 10 MW/m^2, consistent with the earlier 100% argon experiments [Fig. 6]. However, in both substrate cases,

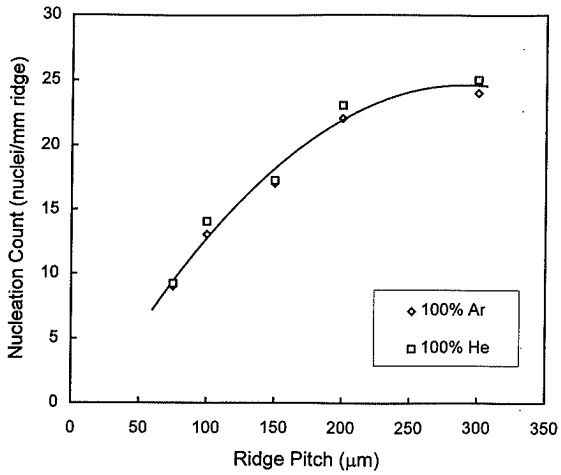

Fig. 13. The effect of substrate surface textures on the nucleation count along the ridges for samples solidified using argon and helium gas atmospheres.

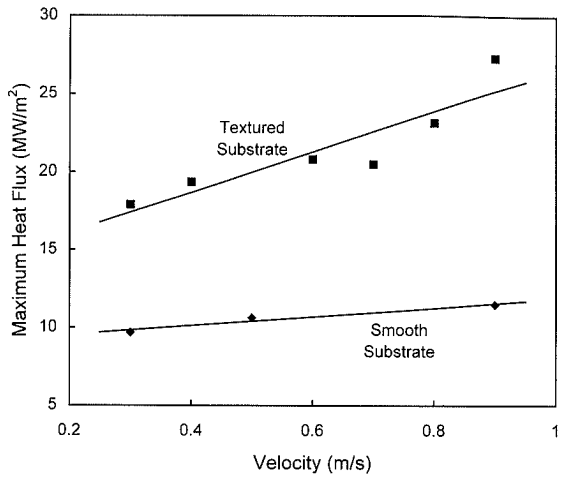

Fig. 14. The effect of immersion velocity on the maximum heat flux for samples solidified on smooth and textured substrates.

there was a significant increase in maximum heat flux with increasing helium; replacing argon completely by helium enhanced the peak heat flux by about 5 MW/m^2.

The surface structures with increasing helium content, however, exhibited the same characteristics as the ones produced in argon atmospheres and no significant differences could be found. The nucleation frequencies on the textured substrate with helium were therefore measured and compared with the argon data shown earlier [Fig. 9]. The averaged nucleation frequency along the ridges as a function of the ridge pitch and the gas atmosphere is summarised in **Fig. 13**.

The nucleation frequency per unit of ridge length increased significantly with increasing ridge pitch, but was only marginally affected by the change from argon to helium. This indicates that the effectiveness and intimacy of direct melt/substrate contacting was dominated by the surface texture and not influenced by the gas atmosphere. The enhanced heat transfer with helium [Fig. 12] could therefore only be due to the higher heat conduction rates through the gas trapped at the melt/substrate interfacial gap and the valleys of the ridge texture.

3.3. Immersion Velocity

The objective of these experiments was to examine the effect of substrate immersion velocity on interfacial heat transfer. The substrates selected for these experiments were one with a smooth surface and one with a ridged surface texture of 75 μm pitch. Melt superheat was maintained at 75 degrees and an argon furnace gas atmosphere was employed throughout the experiments. Immersion velocities were varied systematically in the range 0.3 to 0.9 m/s.

The heat transfer data are summarised in **Fig. 14** in the form of the peak heat flux during initial contacting as a function of immersion velocity for the smooth and textured substrates. The maximum heat flux for both substrate surfaces increased with increasing velocity. However, the effect was more pronounced with the textured substrate.

The observed increase in peak heat flux with immersion velocity does imply an improvement in the effectiveness of melt/substrate contact, and this was reflected in finer surface structures and greater nucleation densities with increasing velocity for both substrates. Nucleation frequencies were higher with the textured surface than the smooth, and the nucleation frequency along the ridges was observed to increase with immersion velocity.

Increasing the immersion velocity could be expected to enhance the melt phase convective heat transfer, but this could not account for the measured increase in heat flux, based on heat transfer correlations for liquid metal flow across plates.[11] The mechanism by which immersion velocity enhances the effectiveness of initial contact may be linked to its effect on meniscus shape and dynamic wetting, but this could not be resolved within the present experimental arrangement.

3.4. Melt Superheat

A series of experiments was carried out, in which the melt temperature was systematically varied from 1 460 to 1 550°C, corresponding to a melt superheat range of 10 to 100 degrees. The smooth substrate surface finish was selected for these experiments. The immersion velocity was constant at 0.5 m/s, and the furnace atmosphere was argon. The initial substrate temperature prior to immersion was kept constant throughout the experiments.

Melt superheat was seen to have a significant effect on the peak heat flux in the initial 50 milliseconds of melt/substrate contact, as shown in **Fig. 15**. Increased superheat corresponded to decreased maximum heat fluxes.

The surface solidification structures for all samples were coarse dendritic, as with earlier samples on smooth substrates [Fig. 7], and their coarseness increased with increasing melt superheat. This was supported by nucleation frequency measurements, which showed a strong dependence on the level of superheat. The average nucleation density is presented in **Fig. 16**. Nucleation density decreased with increasing melt superheat, consistent with but more pronounced than the observed decrease in peak heat flux. Any anticipated enhancement

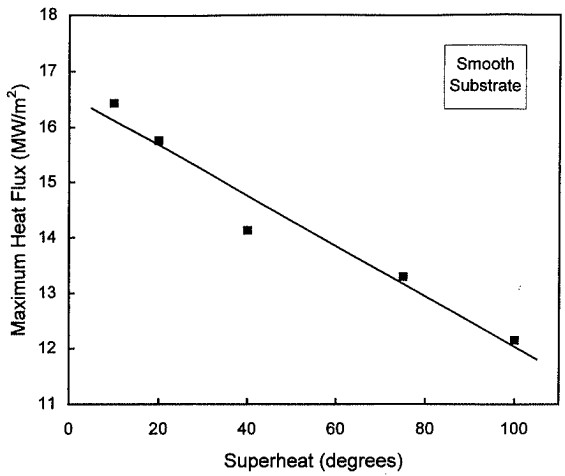

Fig. 15. The effect of melt superheat on the maximum heat flux.

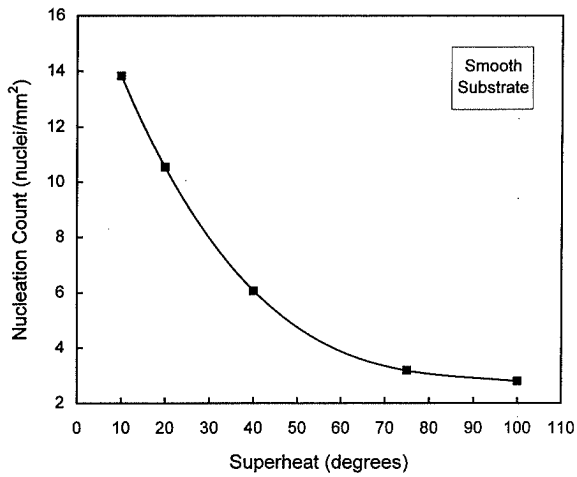

Fig. 16. The effect of melt superheat on nucleation density.

of melt/substrate wetting with increased superheat has presumably been offset by the reduced driving force for nucleation. **Figure 17** shows the close relationship between the calculated maximum heat fluxes and the measured nucleation densities.

Transverse solidification structures of the samples solidified at 10 degrees superheat showed a considerable increase in shell thickness, compared to those at 100 degrees superheat, reflecting the decreased requirement for sensible heat removal. The solidification structure of the samples solidified at 100 degrees superheat were fully columnar. The solidification structures of the samples solidified at 10 degrees melt superheat were partially columnar, with a transition to equiaxed crystals at about one third of the final thickness. This is consistent with the increased tendency for equiaxed growth with reducing superheat.

4. Conclusions

An experimental capability has been developed for studying the fundamentals of interfacial heat transfer and initial solidification, under conditions approximating the meniscus region in strip casting. Transient heat transfer rates have been measured with 0.5 ms resolution

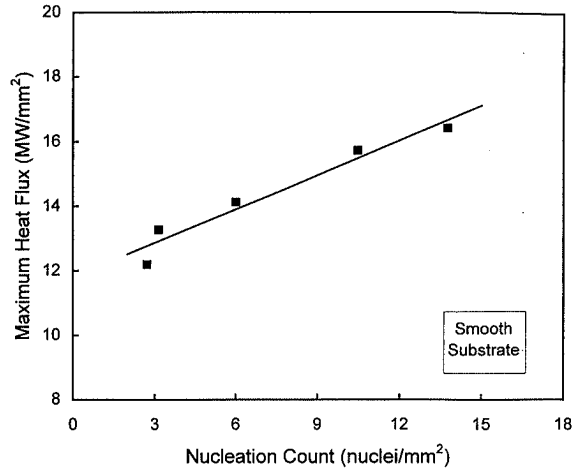

Fig. 17. The correlation between nucleation density and the maximum heat flux.

during the first 50 milliseconds of contact between a stainless steel melt and copper substrates. The heat fluxes were found to rise to a maximum value after about 10 milliseconds, as melt/substrate contact was established. The peak heat flux was a quantitative reflection of the effectiveness of initial melt/substrate contacting, which correlated strongly with nucleation behaviour in the solidified samples. The maximum heat fluxes were higher for textured surfaces than for smooth substrates, and were influenced by the pitch of the ridge textures. Maximum heat fluxes increased with increasing gas phase thermal conductivity, increasing immersion velocity and decreasing melt superheat. Nucleation and surface solidification was aligned with the ridge pattern for textured substrates, compared to the relatively random and coarse nucleation on smooth substrates. Nucleation densities along the length of the ridges increased with ridge pitch for textured substrates, and increased with increasing immersion velocity. Nucleation densities on smooth substrates decreased significantly with increasing superheat. The gas atmosphere enhanced heat transfer across the interfacial gap, but had little effect on the nucleation rates. These results are preliminary, and there exists considerable scope to study different substrate textures and materials as well as different melt compositions and operating variables. However, fundamental studies of this kind should assist in understanding and improving strip surface quality, particularly when interpreted in conjunction with actual performance and quality data from operating strip casting plants or prototypes.

Acknowledgements

BHP Steel, with engineering collaborators IHI, has engaged in a major strip casting program, which is now in the commercial development phase. The funding for this work was provided by BHP Research as part of a collaborative program with University of Newcastle on solidification and casting fundamentals. We would like to thank our many colleagues for technical assistance, discussions and support. In particular, we wish to acknowledge J. Freeman, G. Younger, P. Campbell, R. Mahapatra, G. Belton, H. Fukase and W. Blejde.

REFERENCES

1) J. Birat and R. Steffen: *Metall. Plant Technol. Int.*, **5** (1991), 44.
2) T. Mizoguchi and K. Miyazawa: Proc. of the First European Conf. on Advanced Materials and Processes, Vol. 1, (1989), 93.
3) K. Miyazawa, T. Mizoguchi, Y. Ueshima and S. Mizoguchi: Int. Conf. on New Smelting Reduction and Near Net Shape Casting Technologies for Steel, Vol. 2, Pohang, Korea, (1990), 745.
4) T. Mizoguchi, K. Miyazawa and Y. Ueshima: *Tetsu-to-Hagané*, **80** (1994), 36.
5) T. Mizoguchi, K. Miyazawa and Y. Ueshima: *ISIJ Int.*, **36** (1996), 417.
6) J. C. Grosjean, J. L. Jacquot, J. M. Damasse, H. Littersheidt, D. Senk and W. Schmitz: *Iron Steelmaker*, August, (1993), 27.
7) R. E. Maringer: Casting of Near Net Shape Products, The Metallurgical Society, (1988), 351.
8) A. Morales, M.E. Glicksman and H. Biloni: "Solidification and Casting of Metals", Proc. of Int. Conf. Sheffield, (1977), 184.
9) K. A. Woodbury: *Int. J. Heat Mass Transfer*, **33** (1990), No. 12, 2641.
10) J. V. Beck, B. Blackwell and C. R. St. Clair: Inverse Heat Conduction: Ill-Posed Problems, John Wiley and Sons, New York, (1985).
11) B. Lubarsky and S.J. Kaufman: NACA TN (1955), 3336.